Journal of Sound and Vibration (2000) **236**(5), 801–831
doi:10.1006/jsvi.2000.3002, available online at http://www.idealibrary.com on IDEAL®

ERRORS IN THE MEASUREMENT OF ACOUSTIC ENERGY DENSITY IN ONE-DIMENSIONAL SOUND FIELDS

BEN S. CAZZOLATO† AND COLIN H. HANSEN

Department of Mechanical Engineering, University of Adelaide, SA, 5005, Australia

(*Received* 4 *June* 1999, *and in final form* 25 *February* 2000)

Acoustic energy density has been shown previously to be an effective cost function for active control of noise in enclosed sound fields. Here bias errors in the energy density measurements that occur in one-dimensional sound fields when using the two-microphone technique to estimate the particle velocity are discussed. Four types of bias error for both two- and three-microphone arrangements are investigated; namely, inherent, phase mismatch, sensitivity mismatch and spatial errors.

1. INTRODUCTION

To overcome the observability difficulties that are inherent with microphones as error sensors for the active control of enclosed sound fields, Sommerfeldt and Nashif [1] suggested minimizing the energy density at discrete locations. Energy density is the sum of the acoustic potential and kinetic energies and can be used as an alternative to measuring the pressure at a point. In a numerical simulation Sommerfeldt and Nashif [1] found that minimization of the energy density at a discrete location significantly outperformed the minimization of squared pressures.

There is very little published literature about the sensor systems and the errors arising from the measurement of energy density, especially with regard to its use in active control systems. However, a great deal has been written about measuring acoustic intensity [2–12], a detailed summary of which may be found in Fahy [13]. Much of this literature is directly relevant to the measurement and error analysis of energy density sensors as will be seen later.

According to Fahy [13], measurement of acoustic intensity and thus acoustic energy density is subject to errors associated with the following factors: approximations in the assumed relations between the directly transduced quantities and the energy density (inherent errors): imperfections in the sensor transducers; imperfections in the signal processor in its function of converting the acquired analogue signals into the quantities required to compute energy density; errors of calibration; variations of transducer sensitivity from the calibration value caused by environmental conditions; "noise" produced either by non-acoustic disturbances, such as turbulent airflow, or by the instrument itself.

The measurement of sound intensity and energy density requires estimates of both the pressure and particle velocity. A microphone is almost exclusively used to measure the

† Now at the Institute of Sound and Vibration Research, University of Southampton, Southampton SO17 1BJ, England.

0022-460X/00/400801 + 31 $35.00/0

pressure; however, measurement of the particle velocity is not as simple. The most common technique of estimating the particle velocity is the *two-microphone technique* which uses two separated microphones to estimate the gradient at the midpoint of the two elements, from which the particle velocity can be calculated. The mean pressure is generally used as the "sensor pressure".

There are three distinct sources of error which occur when estimating acoustic energy density using the two-microphone technique; finite separation (inherent) errors, diffraction and interference effects at the microphones, and instrumentation errors. The inherent errors act to limit the upper frequency range of the sensor and the instrumentation errors such as magnitude and phase mismatches act to restrict the low-frequency limit.

The purpose of the following error analysis is to gain some primary understanding of the errors that may arise during the measurement of energy density using the two-microphone technique. It will be shown that the errors in both the pressure and particle velocity components of the energy density will act to bias the overall energy density estimate. Therefore, the following error analysis will investigate the effects of errors on the pressure, particle velocity and energy density for one-dimensional sound fields. The errors arising from energy density measurement using three-dimensional sensors are to be presented in a companion paper [14].

By considering one-dimensional sound fields, there is a simple analytical solution to what for three-dimensional sound fields becomes an extremely complex expression [14] and it is not a trivial task to draw conclusions from the 3-D analysis that are applicable to the 1-D case. In addition, one-dimensional sound fields probably form the most successful environment for active noise control (ANC) system in practice. Thus, it is important that the 1-D case be treated separately, particularly because of the potential application to active control of noise propagating in ducts.

The principles of energy density measurement and the errors arising in the measurement of acoustic energy density will now be derived for measurement in one-dimensional sound fields. The work presented here is a summary of the errors, the derivations for which can be found elsewhere [15].

2. PRINCIPLES OF ACOUSTIC ENERGY DENSITY MEASUREMENT

The instantaneous acoustic energy density $E_D(t, \mathbf{x})$ at some point $\mathbf{x}$, is given by the equation [16]

$$E_D(t, \mathbf{x}) = \frac{p^2(t, \mathbf{x})}{2\rho c^2} + \frac{\rho v^2(t, \mathbf{x})}{2}, \tag{1}$$

where $p(t, \mathbf{x})$ and $v(t, \mathbf{x})$ are the instantaneous pressure and particle velocity, respectively, at $\mathbf{x}$, c is the speed of sound and ρ is the density of the fluid. The instantaneous particle velocity in a one-dimensional sound field is given by Euler's equation

$$v(t, \mathbf{x}) = -\frac{1}{\rho} \int \frac{\partial p(t, \mathbf{x})}{\partial x} \, \mathrm{d}t. \tag{2}$$

In practice, it is very difficult to measure directly the particle velocity and it is generally estimated using a two-microphone finite difference approximation of the pressure gradient [13] as shown in Figure 1.

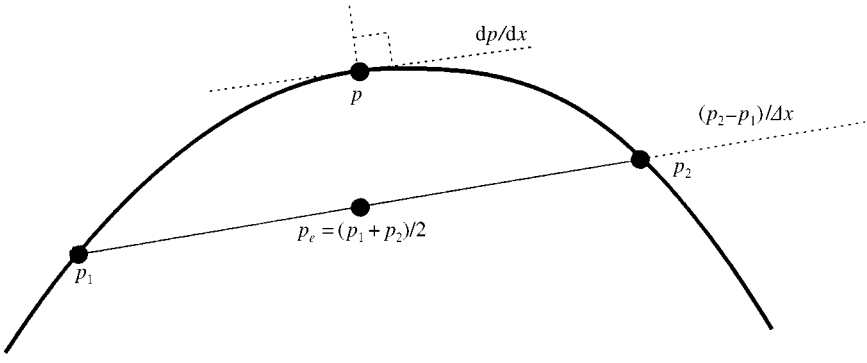

Figure 1. Illustration of the estimation of the particle velocity and pressure from the two-microphone technique. Typically, the sound pressure estimate shows greater error than the particle velocity estimate.

The finite difference approximation for the pressure gradient between two points $\mathbf{x}_1$ and $\mathbf{x}_2$ is

$$\nabla_{xx} p(t, \mathbf{x}) \approx \frac{p(t, \mathbf{x}_2) - p(t, \mathbf{x}_1)}{\Delta x}. \tag{3}$$

Using the finite difference approximation, equation (2) can be re-written as

$$v(t, \mathbf{x}) \approx -\frac{1}{2h\rho} \int [p(t, \mathbf{x}_2) - p(t, \mathbf{x}_1)]\, \mathrm{d}t, \tag{4}$$

where $2h$ is the distance separating the acoustic centres of the microphones, commonly referred to as the *separation distance*. The pressure at the point midway between the microphones is approximated by the finite sum

$$p(t, \mathbf{x}) \approx \frac{p(t, \mathbf{x}_1) + p(t, \mathbf{x}_2)}{2}. \tag{5}$$

Hence, the instantaneous acoustic energy density using two microphones is approximated by

$$E_D(t, \mathbf{x}) \approx \frac{[p(t, \mathbf{x}_1) + p(t, \mathbf{x}_2)]^2}{8\rho c^2} + \frac{[\int [p(t, \mathbf{x}_2) - p(t, \mathbf{x}_1)]\, \mathrm{d}t]^2}{8\rho h^2}. \tag{6}$$

From equation (1) the time-averaged acoustic energy density at $\mathbf{x}$ is given by

$$\bar{E}_D(\mathbf{x}) = \frac{\bar{p}^2(\mathbf{x})}{2\rho c^2} + \frac{\rho \bar{v}^2(\mathbf{x})}{2} = \frac{1}{2\rho c^2} [\bar{p}^2(\mathbf{x}) + (\rho c \bar{v})^2(\mathbf{x})], \tag{7}$$

where $\bar{p}$ and $\bar{v}$ are the time-averaged acoustic pressure and particle velocity at $\mathbf{x}$ respectively.

3. ERRORS IN THE MEASUREMENT OF ACOUSTIC ENERGY DENSITY IN 1-D

The following error analysis for acoustic energy density has drawn heavily from the work of Fahy [13] and others [2–12] regarding errors in sound intensity measurements.

It will be seen that sensing energy density is significantly more tolerant of instrumentation errors than sensing sound intensity. This is because the calculation of sound intensity requires the product between the pressure and particle velocity to be taken, and when these are in quadrature or close to quadrature, such as in a reactive sound field, any small error in phase between the pressure and particle velocity leads to a large error in the active sound intensity. The calculation of acoustic energy density takes the sum of the squares of the pressure and particle velocity, and therefore is only susceptible to errors in magnitudes of the two components.

As was discussed earlier, there are three distinct sources of error which occur when estimating acoustic energy density using the two-microphone technique; namely, finite separation (inherent) errors, diffraction and interference effects at the microphones, and instrumentation errors.

The following errors will now be analyzed for a one-dimensional sound field.

Inherent errors arise due to finite sum and finite difference approximations used to estimate the pressure and particle velocity respectively.

Phase error is an instrumentation error and is due to phase mismatches between microphone pairs which occur commonly in practice.

Sensitivity error is also an instrumentation error and arises from sensitivity mismatches between microphone pairs.

Length error is another form of instrumentation error, but unlike the phase and sensitivity error which arise from transduction and electrical sources, the length error is due to errors in the physical construction of the sensor.

Diffraction and interference effects arise from the finite size of the body housing the microphones.

Other errors including the effect of mean flow and turbulence, environmental effects such as humidity and temperature and statistical or random errors.

3.1. FINITE SEPARATION (INHERENT) ERRORS

According to Fahy [13], the two-microphone technique used for the transduction of sound pressure and particle velocity is subject to systematic errors which arise from the fact that they involve approximations, namely equations (4) and (5). The inherent errors are functions of the type of field under investigation and the orientation and position of the sensor within the field. The implication of this fact is that the magnitude of the inherent error can never be precisely estimated in an arbitrary sound field. Therefore, examples of errors in a range of idealized sound fields are presented to provide an indication of their sensitivity to the parameters of the field and of the sensor.

The following analysis applies to a one-dimensional sound field with spatial variation in the direction of the sensor, which for convenience will be denoted x. According to the Taylor series expansion [13], the pressure at a point is given by

$$p(x+h,t) = p(x,t) + hp^{(1)}(x,t) + (h^2/2)p^{(2)}(x,t) + (h^3/6)p^{(3)}(x,t) + \cdots$$

$$+ (h^n/n!)p^{(n)}(x,t) + \cdots, \tag{8}$$

where $p^{(n)}(x,t)$ denotes the nth derivative of p with respect to x at any time t.

Consider a pair of microphones for which the acoustic centres are separated by a distance $2h$ as shown in Figure 1. Equation (5) gives the estimated pressure at a point midway

between the transducer centres as

$$p_e(t) = \frac{p(x+h) + p(x-h)}{2}$$

$$= p(t) + (h^2/2)p^{(2)}(t) + (h^4/24)p^{(4)}(t) + \cdots + (h^{2n}/2n!)p^{(2n)}(t) + \cdots \tag{9}$$

in which explicit indication of spatial position has been omitted for simplicity in notation. From equation (4), the estimated axial particle velocity component at the centre of the sensor is given by

$$v_e(t) = -\frac{1}{2\rho h}\int [p(x-h) - p(x+h)]\,\mathrm{d}t$$

$$= -\frac{1}{\rho}\int_{-\infty}^{t} [p^{(1)}(\tau) + (h^2/6)p^{(3)}(\tau) + (h^4/120)p^{(5)}(\tau) + \cdots]\,\mathrm{d}\tau \tag{10}$$

The normalized errors in the estimates of p and v, are obtained by dividing the estimate (be it pressure or velocity) by the exact measurement and subtracting 1, i.e.,

$$e(p) = (p_e - p)/p \tag{11}$$

and

$$e(v) = (v_e - v)/v. \tag{12}$$

Substituting the Taylor series expansions for the pressure and particle velocity, given by equations (9) and (10), into the expressions for the normalized errors, given by equations (11) and (12), results in

$$e(p) = [(h^2/2)p^{(2)}(t) + (h^4/24)p^{(4)}(t) + \cdots]/p(t) \tag{13}$$

and

$$e(v) = \frac{\displaystyle\int_{-\infty}^{t} [(h^2/6)p^{(3)}(\tau) + (h^4/120)p^{(5)}(\tau) + \cdots]\,\mathrm{d}\tau}{\displaystyle\int_{-\infty}^{t} p^{(1)}(\tau)\,\mathrm{d}\tau}. \tag{14}$$

These expressions can only be evaluated if the time history of p and of its spatial derivatives are known, which is the case with harmonic field. Thus, this error analysis is not applicable to random sound fields.

Consider a harmonic field defined by, $p(x,t) = \Re\{P(x)\mathrm{e}^{\mathrm{j}\omega t}\}$ and $v(x,t) = \Re\{V(x)\mathrm{e}^{\mathrm{j}\omega t}\}$; the explicit indication of x-dependence has been omitted. Now, the complex velocity magnitude is

$$V = (\mathrm{j}/\omega\rho)P^{(1)} \tag{15}$$

and the complex velocity estimate is

$$V_e = -(\mathrm{j}/2\omega\rho h)(P_1 - P_2) \tag{16}$$

and the normalized error in the velocity estimate is given by

$$e(v) = \frac{[(h^2/6)P^{(3)} + (h^4/120)P^{(5)} + \cdots]}{P^{(1)}}. \tag{17}$$

From equation (7) the estimated time-averaged acoustic energy density is approximated by

$$\bar{E}_{D_e} \approx \frac{[P_1 + P_2][P_1 + P_2]^*}{16\rho c^2} + \frac{[P_2 - P_1][P_2 - P_1]^*}{16\rho\omega^2 h^2}. \tag{18}$$

The Taylor series expansion of the time-averaged energy density estimate is [15]

$$\begin{aligned}\bar{E}_{D_e} = {} & \frac{1}{4\rho c^2}\left[PP^* + \frac{h^2}{2}(P^*P^{(2)} + PP^{(2)*}) + \frac{h^4}{4}\left(P^{(2)*}P^{(2)} + \frac{PP^{(4)*}}{6} + \frac{P^*P^{(4)}}{6}\right)\right] \\ & + \frac{1}{4\rho\omega^2}\left[P^{(1)}P^{(1)*} + \frac{h^2}{6}(P^{(1)*}P^{(3)} + P^{(1)}P^{(3)*})\right. \\ & \left. + \frac{h^4}{12}\left(\frac{P^{(3)*}P^{(3)}}{3} + \frac{P^{(1)}P^{(5)*}}{10} + \frac{P^{(1)*}P^{(5)}}{10}\right)\right].\end{aligned} \tag{19}$$

The exact time-averaged energy density is given by

$$\bar{E}_D = \frac{PP^*}{4\rho c^2} + \frac{\rho VV^*}{4}. \tag{20}$$

Substituting equation (15) into the above equation gives

$$\bar{E}_D = \frac{PP^*}{4\rho c^2} + \frac{P^{(1)}P^{(1)*}}{4\rho\omega^2} = \frac{1}{4\rho c^2}\left(PP^* + \frac{P^{(1)}P^{(1)*}}{k^2}\right). \tag{21}$$

The normalized error in the energy density is given by

$$e(\bar{E}_D) = (\bar{E}_{D_e} - \bar{E}_D)/\bar{E}_D. \tag{22}$$

Therefore, the Taylor series expansion of the normalized time-averaged energy density error is

$$\begin{aligned}e(\bar{E}_D) = {} & \left[\frac{h^2}{2}(P^*P^{(2)} + PP^{(2)*}) + \frac{h^4}{4}\left(P^{(2)*}P^{(2)} + \frac{PP^{(4)*}}{6} + \frac{P^*P^{(4)}}{6}\right)\right] \Bigg/ \left(PP^* + \frac{P^{(1)}P^{(1)*}}{k^2}\right) \\ & + \frac{1}{k^2\left(PP^* + \frac{P^{(1)}P^{(1)*}}{k^2}\right)} \\ & \times \left[\frac{h^2}{6}(P^{(1)*}P^{(3)} + P^{(1)}P^{(3)*}) + \frac{h^4}{12}\left(\frac{P^{(3)*}P^{(3)}}{3} + \frac{P^{(1)}P^{(5)*}}{10} + \frac{P^{(1)*}P^{(5)}}{10}\right)\right].\end{aligned} \tag{23}$$

In the future, when referring to the normalized energy density error the reference to time-averaged will be omitted for brevity.

Although not immediately obvious from the above expression it will be shown in the following two sections that in general the majority of the inherent error comes from the finite sum approximation of the pressure rather than the finite difference approximation used for the particle velocity. This is also the case when measuring sound intensity [12]. It is therefore interesting to consider the case of a three-microphone energy density sensor where the centre microphone measures the pressure at the centre of the sensor as seen in Figure 2. The additional microphone does not increase the accuracy of the finite difference approximation. Consequently, in this latter arrangement, all the inherent error is due to the velocity approximation and although the error is still in the order of $(kh)^2$ the error is substantially reduced.

The inherent energy density error for a three-microphone sensor in a reactive one-dimensional sound field is given by the second term in equation (23), i.e.,

$$e(E_{D_3}) \approx \frac{1}{k^2(PP^* + P^{(1)}P^{(1)*}/k^2)} \times \left[\frac{h^2}{6}(P^{(1)*}P^{(3)} + P^{(1)}P^{(3)*}) + \frac{h^4}{12}\left(\frac{P^{(3)*}P^{(3)}}{3} + \frac{P^{(1)}P^{(5)*}}{10} + \frac{P^{(1)*}P^{(5)}}{10}\right)\right]. \quad (24)$$

It should be noted that the previous derivations are valid for any type of one-dimensional sound field and may be used to calculate the resulting errors that would arise from a one-dimensional energy density sensor in any one-dimensional environment. The errors associated with two common idealized sound fields models are now analyzed, namely; a one-dimensional reactive sound field and a plane progressive wave. The reasons for choosing the two extremes of acoustic environment to demonstrate the error analysis are as follows: although most ANC applications tend to be in sound fields that are neither purely plane progressive waves nor reactive, the most successful applications do tend to occur when the system is almost reactive or almost free field. For example, in heavily damped reactive cavities, it is extremely difficult to achieve global control throughout the enclosure. Therefore, since the most successful ANC systems are found in either very lightly damped reactive enclosures or free-field conditions it was considered that these were best approximated by the two extremes just discussed.

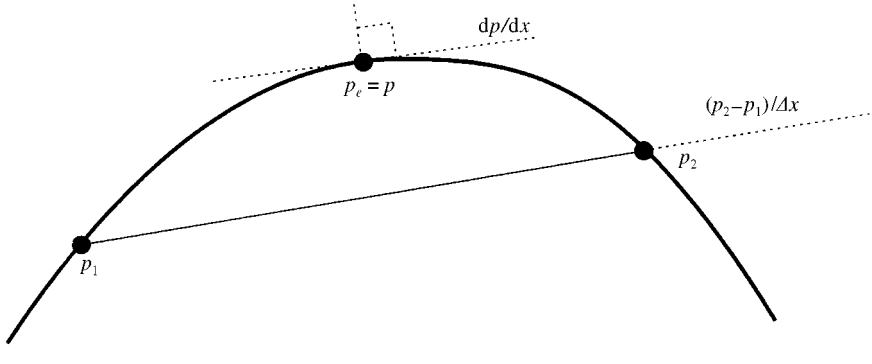

Figure 2. Particle velocity from the two-microphone technique with an additional centre microphone.

3.1.1. *One-dimensional reactive sound field*

The sound field which exhibits greatest variation in the acoustic potential energy is a cavity with a single mode excited. This situation is commonly encountered in low modal density cavities and poses significant problems when using microphones as error sensors.

For a harmonic sound field of frequency, ω, in which $p(x,t) = \Re\{P(x)e^{j\omega t}\}$ and $v(x,t) = \Re\{V(x)e^{j\omega t}\}$, consider a stationary reactive sound field defined by the following:

$$p(x,t) = P_0 \cos(k_l x)\,\Re\{e^{j\omega t}\} = P_0 \cos(k_l x)\cos(\omega t), \tag{25}$$

where ω is the driving frequency of the sound and k_l is the eigenvalue of the mode given by $k_l = n\pi/L$, where n is an integer and L is the length of the cavity. The velocity corresponding to a point x_0 is given by

$$v(x_0,t) = -\frac{1}{\rho}\int \frac{\partial P(x_0)}{\partial x}\,dt = \frac{P_0 k_l}{\rho\omega}\sin(k_l x_0)\sin(\omega t). \tag{26}$$

For the sound field given by equation (25) the exact energy density throughout the acoustic space is

$$E_D = \frac{P_0^2}{4\rho c^2}. \tag{27}$$

The pressure and pressure gradients are given by

$$P = P_0 \cos(k_l x), \qquad P^{(1)} = -k_l P_0 \sin(k_l x), \tag{28, 29}$$

$$P^{(2)} = -k_l^2 P_0 \cos(k_l x) = -k_l^2 P, \qquad P^{(3)} = k_l^3 P_0 \sin(k_l x) = -k_l^2 P^{(1)}. \tag{30, 31}$$

To investigate the effect of wavelength on the accuracy of the estimates it is prudent to let the length of the cavity increase with frequency such that $L = n\lambda/2$, i.e., $k_l = k$. This then allows a direct comparison with the case of a free propagating wave. The normalized errors for the pressure, velocity and energy density are given by equations (11), (12) and (22). For a reactive sound field the pressure, velocity [13, section 5.6.1] and energy density [15] errors are given by

$$e(p) = \cos(kh) - 1 \approx -\frac{(kh)^2}{2} + \frac{(kh)^4}{24} - \frac{(kh)^6}{720} + \cdots, \tag{32}$$

$$e(v) = \frac{\sin(kh)}{kh} - 1 \approx -\frac{(kh)^2}{6} + \frac{(kh)^4}{120} - \frac{(kh)^6}{5040} + \cdots, \tag{33}$$

$$e(E_D) = -(kh)^2\left[\frac{2\cos^2(kx)+1}{3}\right] + (kh)^4\left[\frac{13\cos^2(kx)+2}{45}\right] - \cdots. \tag{34}$$

Note that the normalized error in the estimate of the pressure is approximately three times that of the normalized error in the velocity. By differentiating the above expression for the energy density with respect to x and setting the derivative to zero, the maximum and

minimum error can be found. It can be shown that the zero gradient occurs at $\sin(2kx) = 0$, i.e., $kx = n\pi/2$, with the maximum error found at $kx = n\pi$ and the minimum error at $kx = (2n + 1)\pi/2$. Therefore, the maximum and minimum are given, respectively, by

$$e(E_D)_{max} = -(kh)^2 + \frac{(kh)^4}{3} - \cdots, \quad kx = n\pi,$$

$$e(E_D)_{min} = -\frac{(kh)^2}{3} + \frac{2(kh)^4}{45} - \cdots, \quad kx = (2n + 1)\pi/2. \tag{35}$$

The first term is the energy density error when the acoustic pressure is at a maximum and the particle velocity is zero. Therefore, the error is all due to the error in the pressure measurement and so the above expression can also be derived by

$$e(E_D)_{max} = \frac{p_e^2 - p^2}{p^2} = (1 + e(p))^2 - 1 = 2e(p) + e^2(p). \tag{36}$$

Likewise, the smallest error in the energy density occurs when the particle velocity is at a maximum (and the pressure is zero) and is given by

$$e(E_D)_{min} = \frac{v_e^2 - v^2}{v^2} = (1 + e(v))^2 - 1 = 2e(v) + e^2(v). \tag{37}$$

For the three-microphone sensor the normalized inherent error is [15]

$$e(E_{D_3}) \approx \sin^2(kx)\left[-\frac{(kh)^2}{3} + \frac{2(kh)^4}{45} - \cdots\right]. \tag{38}$$

For the three-microphone sensor, the energy density error is obviously zero when at a pressure maximum, i.e., $kx = 0$, and has a maximum when at a velocity maximum, i.e., $kx = (2n + 1)\pi/2$, given by the second term in equation (35). Therefore, the additional microphone has reduced the maximum energy density error by a factor of three.

The inherent error for both the two-microphone sensor and the three-microphone sensor are plotted against the non-dimensional separation, $2kh$, for a single-mode reactive sound field and a position to cavity length ratio of $x/L = \frac{1}{4}$ in Figure 3. Obviously, the error for the pressure, velocity and energy density vary with position so it is necessary to select some position which typifies the error as a function of non-dimensional separation. $x/L = \frac{1}{4}$ was chosen since the magnitude of the pressure and velocity are equal at this location.

3.1.2. *Plane progressive wave*

The errors arising from finite separation measurements in a plane wave will now be derived. Consider a plane wave defined by

$$p(x, t) = \Re\{P_0 e^{j\omega t - jkx}\}. \tag{39}$$

The pressure and gradients are given by

$$P = P_0 e^{-jkx}, \qquad P^{(1)} = -jkP, \tag{40, 41}$$

$$P^2 = -k^2 P, \qquad P^3 = jk^3 P = -k^2 P^{(1)}. \tag{42, 43}$$

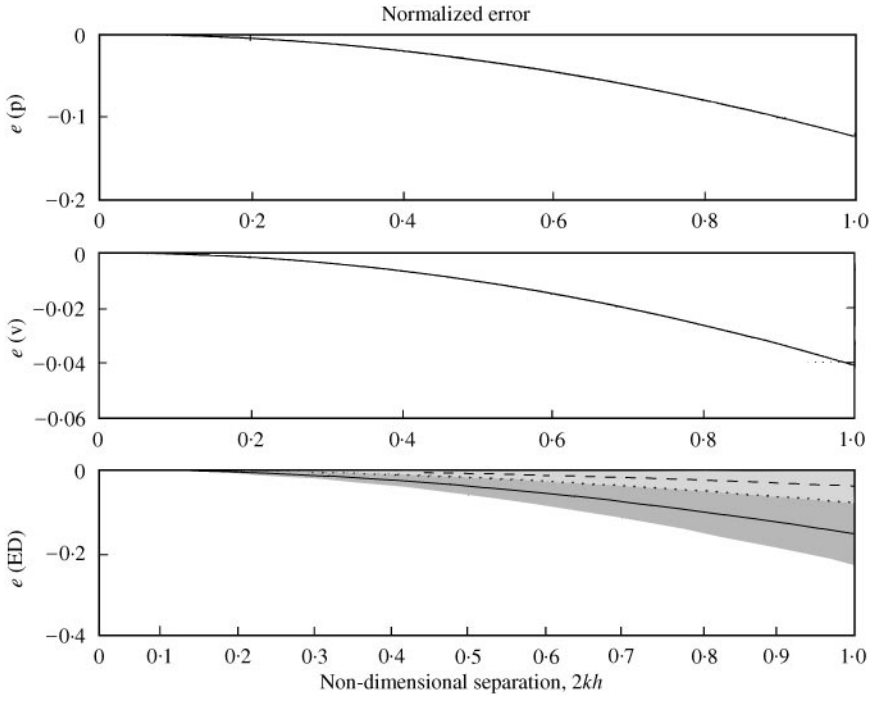

Figure 3. Inherent errors as a function of the non-dimensional separation distance ($2kh$) for a reactive one-dimensional sound field with $x/L = 1/4$: (a) pressure error, $e(p)$ which is zero for the three-microphone sensor; (b) particle velocity error, $e(v)$ which is the same for both sensors; (c) energy density error, $e(ED)$. Maximum and minimum energy density error bands are shaded for the two-microphone sensor (dark grey) and the three-microphone sensor (light grey): —— 2-mic sensor; ---- 3-mic sensor.

It can be shown [13] that the energy density in a plane progressive sound field is given by

$$E_D = \frac{P_0^2}{2\rho c^2}. \tag{44}$$

It is interesting to note that the energy density in a plane progressive sound field is twice that in a one-dimensional reactive sound field. The normalized errors for the pressure, velocity [13] and energy density [15] are given by

$$e(p) = \cos(k_l h) - 1 \approx -\frac{(k_l h)^2}{2} + \frac{(k_l h)^4}{24} - \frac{(k_l h)^6}{720} + \cdots, \tag{45}$$

$$e(v) = \frac{\sin(kh)}{kh} - 1 \approx -\frac{(kh)^2}{6} + \frac{(kh)^4}{120} - \frac{(kh)^6}{5040} + \cdots, \tag{46}$$

$$e(E_D) = -\frac{2}{3}(kh)^2 + \frac{17}{90}(kh)^4 - \cdots. \tag{47}$$

Therefore, the error in the energy density measurement for a progressive sound field is independent of position as one would expect. Note that the first term in the error is the same as that for the error in intensity when using the two-microphone technique [13].

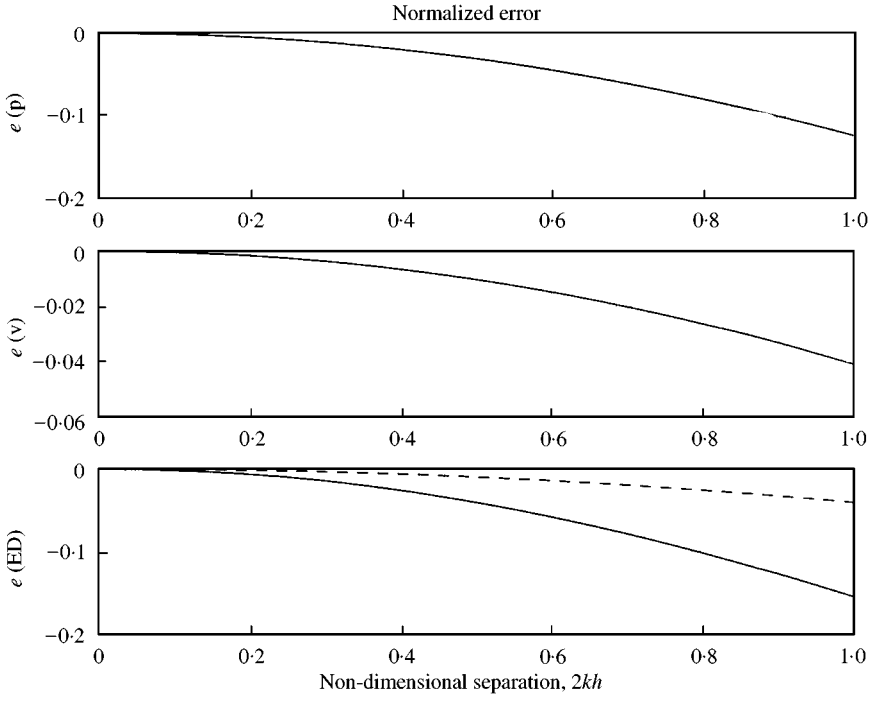

Figure 4. Inherent errors as a function of the non-dimensional separation distance ($2kh$) for a plane progressive wave: (a) pressure error, $e(p)$ which is zero for the three-microphone sensor; (b) particle velocity error, $e(v)$ which is the same for both sensors; (c) energy density error, $e(ED)$: —— 2-mic sensor; - - 3-mic sensor.

For the three-microphone sensor the normalized inherent error for a plane progressive wave is

$$e(E_{D_3}) \approx -\tfrac{1}{6}(kh)^2 + \tfrac{1}{45}(kh)^4 - \cdots. \tag{48}$$

The use of the additional microphone has therefore reduced the normalized error by a factor of 4, compared to a factor of 3 in a reactive sound field.

The inherent error for both the two-microphone sensor and the three-microphone sensor are plotted against the non-dimensional separation, $2kh$, for a progressive plane wave in Figure 4.

3.2. INSTRUMENTATION ERRORS

The two most common instrumentation errors are differences in the transducer transfer functions, commonly referred to as *linear distortion*. Matching the transfer functions (both amplitude and phase responses) of the microphones is of vital importance, particularly at low frequencies where the actual phase difference of the sound pressures is small.

3.2.1. *Phase mismatch errors*

The effect of phase response mismatch upon the accuracy of any particular measurement depends on the relative magnitudes of the phase mismatch of the microphone channels and the actual phase difference of the sound pressures at the sensing points; the latter depends

on the nature of the sound field, and the location and orientation of the sensor within the sound field [13]. For example, in a reactive sound field, the actual phase difference between the sensing points varies between kd and 0 as the sensor axis is rotated through 90° from an initial orientation parallel to the direction of energy flux. Therefore, the normalized phase error varies from a finite value to infinity and so does the normalized velocity error.

Figure 5 illustrates the effect of a phase error of $\pm\phi_s$ on the estimates of p and Δp. It can be clearly seen that not only is there an error in the magnitude of the two estimates but a phase error is also introduced. Unlike the significant detrimental effects phase errors have on the measurement of acoustic intensity, phase errors during the measurement of energy density are relatively benign.

Therefore, in the case of simple harmonic fields the pressure responses of the two microphones with a phase mismatch $2\phi_s$ are given by the products of the true pressures with $e^{\pm j\phi_s}$, that is

$$\hat{p}_1(x,t) = p_1(x,t)e^{j\phi_s}, \qquad \hat{p}_2(x,t) = p_2(x,t)\,e^{-j\phi_s}. \tag{49, 50}$$

The actual phase difference between the transducers (for both a plane wave and a single-mode reactive sound field) is $\phi_0 = 2kh$ where $2h$ is the sensor separation distance. It will be shown that the pressure, velocity and energy density errors are a function of the ratio of the phase mismatch error to the actual phase difference, $2\phi_s/\phi_0$.

The effects of phase mismatch will now be analyzed for two types of idealized sound fields.

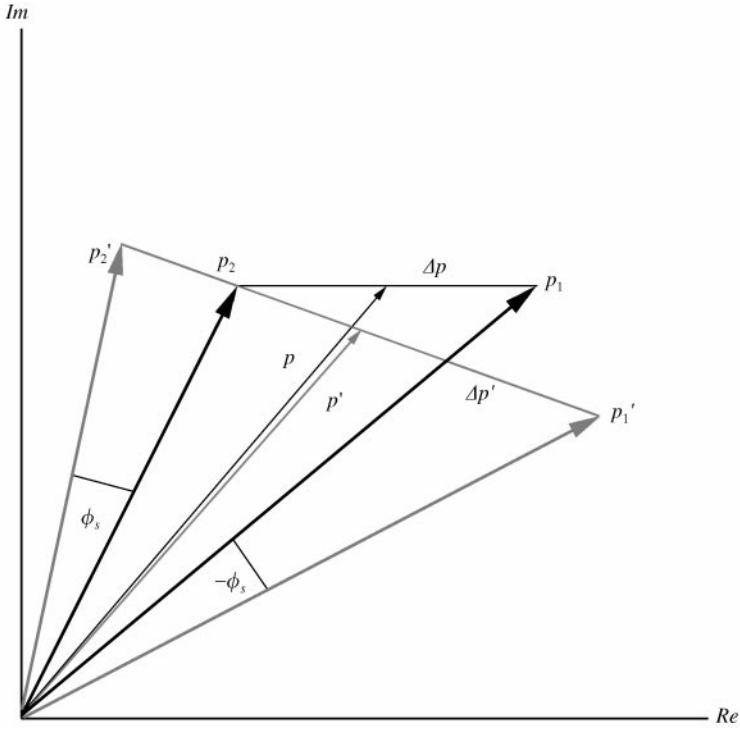

Figure 5. Phasor diagram showing the effect of transducer phase mismatch. Adapted from Fahy [13].

3.2.1.1. One-dimensional reactive sound field. Using the expression for a stationary reactive sound field, equation (25), the mean of the two pressures with a total microphone phase mismatch of $2\phi_s$ is

$$\hat{p}_e = \frac{\hat{p}_1 + \hat{p}_2}{2} = \frac{P_0}{2}[\cos(kx + kh)\cos(\omega t + \phi_s) + \cos(kx - kh)\cos(\omega t - \phi_s)], \quad (51)$$

where the $\hat{}$ represents the pressure response with the phase mismatch. It can be shown that the pressure estimate with the phase error is equal to the pressure estimate without the phase error plus an additional term due to the phase error [15], i.e.,

$$\hat{p}_e = p_e + \alpha_p, \quad (52)$$

where α_p is the additional error due to the phase mismatch, given by

$$\alpha_p = P_0 \phi_s \sin(kx)\sin(kh)\sin(\omega t). \quad (53)$$

Using equation (11) the normalized error for the pressure estimate is given by [15]

$$e(\hat{p}) = e(p) + \mathrm{j}\phi_s \tan(kx)\sin(kh), \quad (54)$$

where $e(p)$ is the normalized pressure error without the phase mismatch arising wholly from the finite sum and is given by equation (32). The additional error in the pressure estimate due to the phase mismatch is zero at $kx = n\pi$ and infinite at $kx = (2n + 1)\pi/2$, that is, when the measurement is made at a pressure node.

As with the pressure estimate, the velocity estimate with the phase error is equal to the velocity estimate without the phase error plus an additional term due to the phase error [15], i.e.,

$$\hat{v}_e = v_e + \alpha_v, \quad (55)$$

where α_v is the additional error due to the phase mismatch given by

$$\alpha_v = \frac{P_0}{\rho\omega}\frac{\phi_s}{h}\cos(kx)\cos(kh)\cos(\omega t). \quad (56)$$

Using equation (21) the normalized error for the velocity estimate is given by [15]

$$e(\hat{v}) = e(v) - \mathrm{j}\frac{\phi_s}{kh}\cot(kx)\cos(kh), \quad (57)$$

where $e(v)$ is the normalized particle velocity error without the phase mismatch arising wholly from the finite difference and is given by equation (33). The additional error in the velocity estimate due to the phase mismatch is zero at $kx = (2n + 1)\pi/2$ and infinite at $kx = n\pi$, that is, when the measurement is made at a velocity node.

The normalized error of the energy density for small kh is therefore, given by [15]

$$e(\hat{E}_D) \approx e(E_D) + \cos^2(kx)\left(\frac{2\phi_s}{2kh}\right)^2, \quad (58)$$

where $e(E_D)$ is the normalized error in the energy density without the phase mismatch arising wholly from the finite separation and is given by equation (34).

Therefore, the normalized error in the energy density arising from the phase mismatch is proportional to the square of the ratio of the phase error to the actual phase difference. From equation (58) it can be seen that the minimum energy density error occurs at $kx = (2n + 1)\pi/2$ and is given by $e(\hat{E}_D)_{min} = e(E_D)$, that is error arising from only the finite separation between the microphones making up the energy density sensor. The maximum error in the energy density estimate is found at $kx = n\pi$ as

$$e(\hat{E}_D)_{max} = e(E_D) + \frac{(2\phi_s)^2}{(2kh)^2}. \tag{59}$$

It is quite clear that the second term in the normalized error dominates the expression as $2kh$ approaches $2\phi_s$, which acts to limit the lowest frequency at which the energy density sensor can be used successfully. It should be noted that the error in the energy density given by equation (58) is independent of the sign of the phase error. The truncated Taylor series expansions for the normalized error in pressure, velocity and energy density as given by equations (54), (57) and (58) using a phase difference of $2\phi_s = 1^\circ$ are plotted against the non-dimensional separation distance in Figure 6 with a non-dimensional position of $x/L = \frac{1}{4}$. The normalized energy density error given by equation (58) is also plotted against the non-dimensional separation distance in Figure 7 for a variety of phase errors.

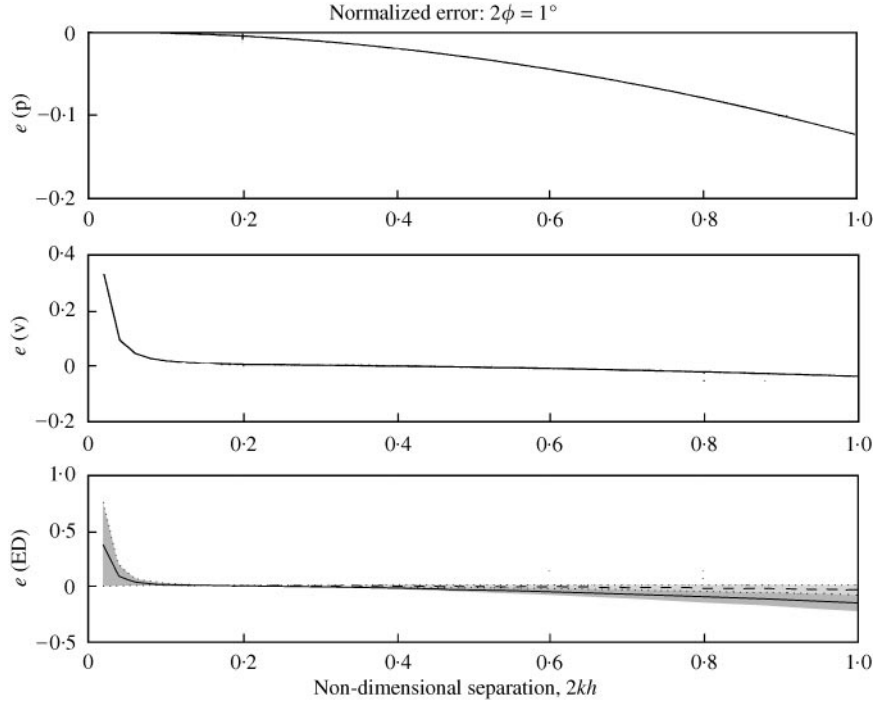

Figure 6. Normalized error in energy density in a reactive one-dimensional sound field as a function of the non-dimensional separation distance ($2kh$) with $x/L = 1/4$: (a) pressure error, $e(p)$ which is zero for the three-microphone sensor; (b) particle velocity error, $e(v)$ which is the same for both sensors; (c) energy density error, $e(ED)$. Maximum and minimum energy density error bands are shaded for the two-microphone sensor (dark grey) and the three-microphone sensor (light grey): —— 2-mic sensor; – – – – 3-mic sensor.

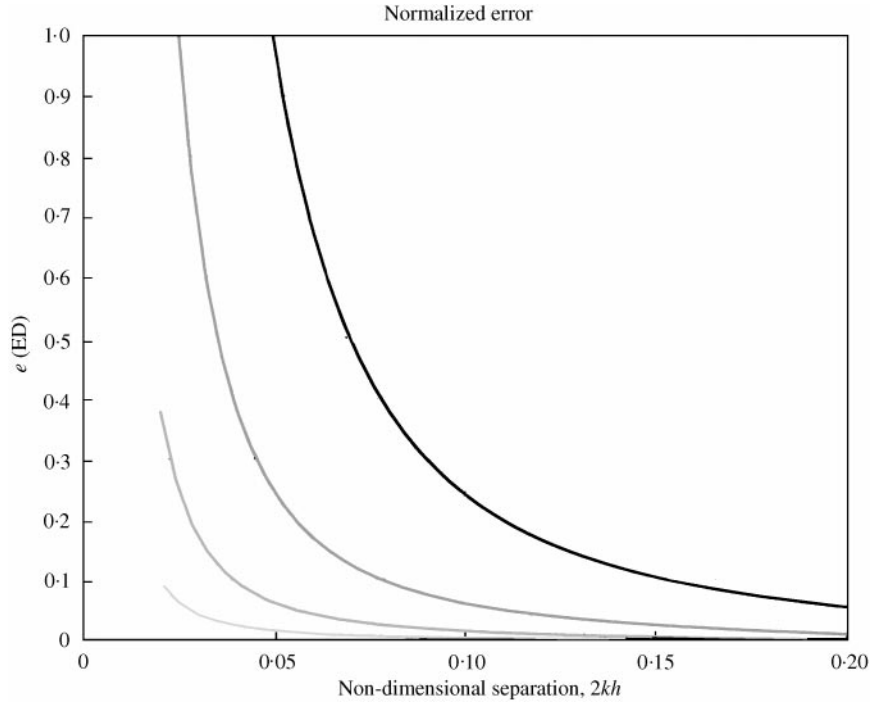

Figure 7. Normalized error in energy density as a function of the non-dimensional separation distance ($2kh$) in a reactive one-dimensional sound field for a variety of transducer phase mismatches with $x/L = 1/4$. For the case of no phase error (0°) there is no significant error in energy density: 0°; 0.5°; 1°; 2°; 4°.

For a three-microphone sensor the normalized error for the pressure is obviously zero, the error for the velocity is the same as given by equation (57) and the normalized error in the energy density is given by equation (58), where $e(E_D) = e(E_{D_3})$ is given by equation (38). Therefore, it can be concluded that although the use of the additional microphone does extend the upper bound at which the sensor can be used, it does not assist in reducing the lower frequency limit.

3.2.1.2. Plane progressive wave. For the case of a plane wave the effect of a phase mismatch is equivalent to modifying the sensor separation distance; i.e., for a phase mismatch of $2\phi_s$ the sensor separation distance is $k\hat{h} = kh - \phi_s$ or $\hat{h}/h = 1 - \phi_s/kh$. The normalized errors for the pressure, velocity [13] and energy density [15] are given by

$$e(p) = \cos(k\hat{h}) - 1 \approx -\frac{(k\hat{h})^2}{2} + \frac{(k\hat{h})^4}{24} - \frac{(k\hat{h})^6}{720} + \cdots, \tag{60}$$

$$e(v) = \frac{\sin(k\hat{h})}{kh} - 1 \approx \left(1 - \frac{\phi_s}{kh}\right)\left(1 - \frac{(k\hat{h})^2}{6} + \frac{(k\hat{h})^4}{120} - \frac{(k\hat{h})^6}{5040} + \cdots\right) - 1, \tag{61}$$

$$e(\hat{E}_D) \approx \frac{1}{2}\left[1 - (k\hat{h})^2 + \frac{1}{3}(k\hat{h})^4\right] + \frac{(1 - \phi_s/kh)^2}{2}\left[1 - \frac{1}{3}(k\hat{h})^2 + \frac{2}{45}(k\hat{h})^4\right] - 1. \tag{62}$$

As kh approaches zero, the normalized error in the energy density approaches

$$e(\hat{E}_D) \approx -\frac{\phi_s}{kh} + \frac{(\phi_s/kh)^2}{2}. \tag{63}$$

The truncated Taylor series expansions for the normalized error in pressure, velocity and energy density as given by equation (60)–(62) using a phase difference of $2\phi_s = -1^\circ$ are plotted against the non-dimensional separation distance in Figure 8. The figure shows that the normalized error in the pressure still approaches zero as kh approaches zero, despite the phase mismatch; however, as the free-field phase difference $2kh$ approaches the phase error ($2\phi_s$), the normalized errors in both the velocity and energy density become significant, increasing at 12 dB per halving in frequency (octave). This is also shown graphically in Figure 9 where the error in energy density given by equation (62) is plotted against non-dimensional separation distance for a variety of phase errors.

For the case of the three-microphone sensor the statement regarding the reactive sound field holds, namely that the error in pressure is zero, the velocity error is the same as for the two-microphone sensor given by equation (61) and the energy density error is given by the second term in equation (62), i.e.,

$$e(\hat{E}_{D_3}) \approx \frac{(1-\phi_s/kh)^2}{2}\left[1 - \frac{1}{3}(k\hat{h})^2 + \frac{2}{45}(k\hat{h})^4\right] - \frac{1}{2}. \tag{64}$$

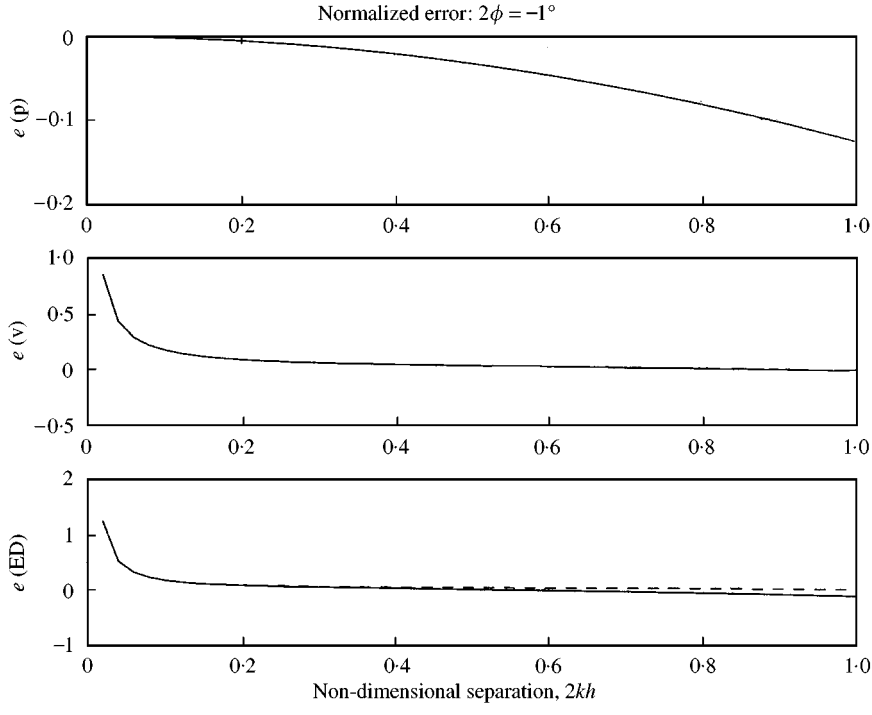

Figure 8. Normalized errors as a function of the non-dimensional separation distance ($2kh$) in a plane wave conditions for a transducer phase mismatch of -1°: (a) pressure error, $e(p)$ which is zero for the three-microphone sensor; (b) particle velocity error, $e(v)$ which is the same for both sensors; (c) energy density error, $e(ED)$: —— 2-mic sensor; – – – – 3-mic sensor.

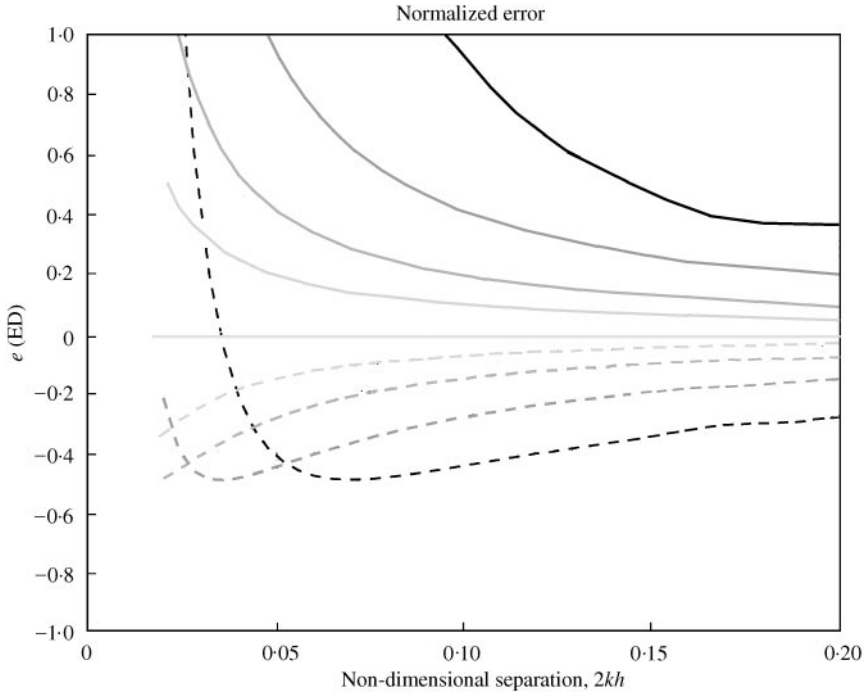

Figure 9. Normalized error in energy density as a function of the non-dimensional separation distance ($2kh$) in a plane wave conditions for a variety of transducer phase mismatches: — $-4°$; — $-2°$; — $-1°$; — $-0.5°$; — $0°$; — $+0.5°$; — $+1°$; — $+2°$; — $+4°$.

3.2.2. *Sensitivity errors*

In addition to phase mismatch, the two microphone sensitivities may differ. The pressure sum and difference are altered in both magnitude and phase by a sensitivity mismatch [13]. The effect is illustrated in Figure 10.

Let the sensitivity difference between the transducers be $\pm T$ such that the ratio of the sensititvities is given by $(1 + T)/(1 - T) \approx 1 + 2T$ for small T, i.e.,

$$\hat{p}_1(x, t) = p_1(x, t)(1 - T), \qquad \hat{p}_2(x, t) = p_2(x, t)(1 + T). \tag{65, 66}$$

The symmetry of the sensitivity error between the two microphone in the above expressions was used in order to simplify the analytical derivation of the errors arising from the sensitivity mismatch. The effects of sensitivity mismatch will now be analyzed for two types of idealized sound field.

3.2.2.1. One-dimensional reactive sound field. Given a stationary reactive sound field defined by the following:

$$p(x, t) = P_0 \cos(kx)\, \Re\{e^{i\omega t}\} = P_0 \cos(kx) \cos(\omega t), \tag{67}$$

where ω and k are the frequency and wavenumber of the sound, respectively, the velocity at a point x_0 is given by

$$v(x_0, t) = -\frac{1}{\rho} \int \frac{\partial p(x_0)}{\partial x}\, dt = \frac{P_0 k}{\rho \omega} \sin(kx_0) \sin(\omega t). \tag{68}$$

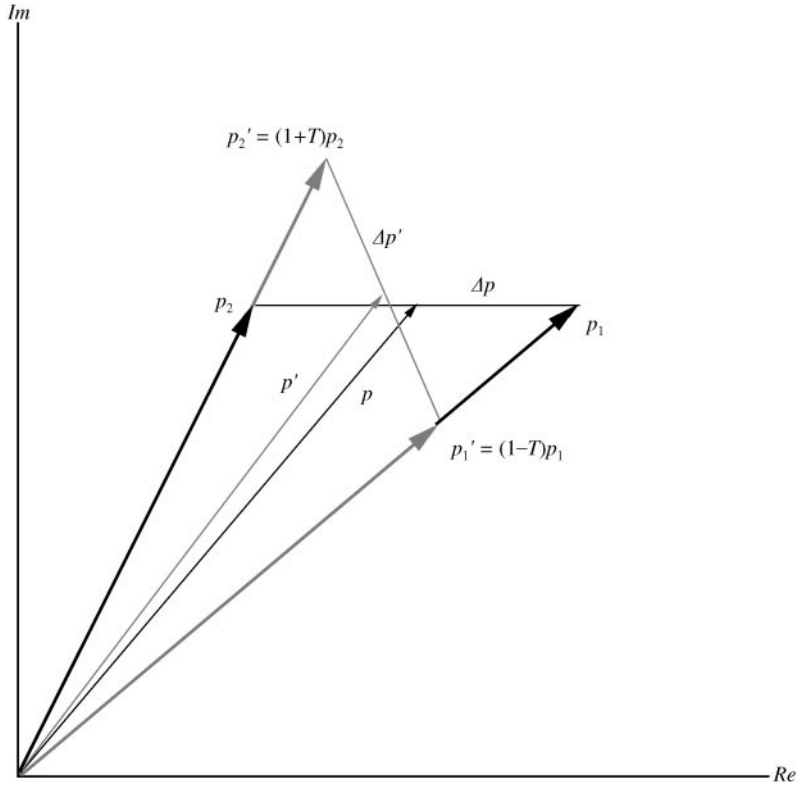

Figure 10. Phasor diagram showing the effect of transducer sensitivity mismatch. Adapted from Fahy [13].

The mean of the two pressures is estimated by two microphones spaced $2h$ apart,

$$\hat{p}_e = \frac{\hat{p}_1 + \hat{p}_2}{2} = \frac{P_0}{2}\left[(1 - T)\cos(kx + kh)\cos(\omega t) + (1 + T)\cos(kx - kh)\cos(\omega t)\right], \quad (69)$$

where the $\hat{}$ represents the pressure response due to the sensitivity mismatch. It can be shown that the pressure estimate with the sensitivity error is equal to the pressure estimate without the sensitivity error, p_e, plus an additional term due to the sensitivity error [15]; i.e.,

$$\hat{p}_e = \frac{\hat{p}_1 + \hat{p}_2}{2} = p_e + \beta_p, \quad (70)$$

where β_p is the additional error due to the magnitude mismatch given by

$$\beta_p = P_0 T \sin(kx)\sin(kh)\cos(\omega t). \quad (71)$$

Therefore, the normalized error of the pressure estimate is [15]

$$e(\hat{p}) = e(p) + T\tan(kx)\sin(kh), \quad (72)$$

where $e(p)$ is the normalized pressure error without the sensitivity mismatch arising wholly from the finite sum approximation and is given by equation (32). It can be seen that the normalized error in the pressure becomes infinite for $kx = \pi/2$. This is because the exact pressure is zero at this location and as a result, any error in the pressure produces an infinite normalized error.

As with the pressure estimate, the velocity estimate is equal to the velocity estimate without the sensitivity error plus an additional term due to the sensitivity error [15], i.e.,

$$\hat{v}_e = v_e + \beta_v, \tag{73}$$

where β_v is the additional error due to the magnitude mismatch given by

$$\beta_v = -\frac{P_0 T}{h\rho\omega}\cos(kx)\cos(kh)\sin(\omega t). \tag{74}$$

The normalized error of the velocity estimate is [15]

$$e(\hat{v}) = e(v) + T\frac{\cos(kh)}{kh\tan(kx)} = \left[\frac{\sin(kh)}{kh} - 1\right] + T\frac{\cos(kh)}{kh\tan(kx)}, \tag{75}$$

where $e(v)$ is the normalized particle velocity error without the sensitivity mismatch arising wholly from the finite difference approximation and is given by equation (33). The additional error in the velocity estimate due to the magnitude mismatch is zero at $kx = (2n+1)\pi/2$ and infinite at $kx = n\pi$, that is, when the measurement is made at a velocity node.

The normalized error in the time-averaged energy density estimate is given by [15]

$$e(\hat{E}_D) = e(E_D) + \frac{2T}{4}\sin(2kx)\sin(2kh)\left(1 - \frac{1}{(kh)^2}\right) + \left(\frac{2T}{2kh}\right)^2\cos^2(kx)\cos^2(kh), \tag{76}$$

where $e(E_D)$ is the normalized error in the energy density without the sensitivity mismatch arising wholly from the finite separation and is given by equation (34).

The first term in the expression is negligible for small sensitivity mismatches and can be ignored. However, the second term is significant and becomes very large as kh decreases. The above equation for small kh can be rewritten as

$$e(\hat{E}_D) \approx e(E_D) - \left(\frac{2T}{2kh}\right)\sin(2kx) + \left(\frac{2T}{2kh}\right)^2\cos^2(kx). \tag{77}$$

Therefore, in order to keep the error in the energy density small, the non-dimensional error in sensitivity $2T$ should be significantly less than the non-dimensional microphone separation $2kh$. From the preceding expression it can be seen that the normalized energy density error at $kx = (2n+1)\pi/2$ (pressure nodes) is given by $e(E_D)$, which is the error arising only from the finite microphone separation. By differentiating the preceding expression for the normalized energy density with respect to x and setting the derivative to zero, the maximum and minimum error can be found. It can be shown that the zero gradient occurs at $\tan(2kx) = -2kh/T$, i.e., $kx = \frac{1}{2}\arctan(-2kh/T) + n\pi/2$, with the

maximum error found at $kx = \frac{1}{2}\arctan(-2kh/T) + n\pi$ and the minimum error at $kx = \frac{1}{2}\arctan(-2kh/T) + (2n+1)\pi/2$.

The truncated Taylor series expansions for the normalized error in pressure, velocity and energy density as given by equations (72), (75) and (76) using a sensitivity difference of $2T = 1\%$ are plotted against the non-dimensional separation distance in Figure 11 with a non-dimensional position of $x/L = \frac{1}{4}$.

The normalized error in the pressure still approaches zero, despite the sensitivity mismatch. However, when the wavenumber becomes small, both the velocity and energy density errors increase at 12 dB per halving in frequency (octave). This is shown graphically in Figure 12 where the error in energy density given by equation (76) is plotted against non-dimensional separation for a variety of sensitivity errors.

For a three-microphone sensor, the pressure error is zero, the velocity error is the same as the two-microphone sensor given by equation (75) and the normalized error in the energy density estimate for small kh is given by equation (76), where $e(E_D) = e(E_{D_3})$ and $e(E_{D_3})$ is given by equation (38).

3.2.2.2. Plane progressive wave. It can be shown that for a plane progressive sound field, the pressure estimate for a sensitivity mismatch is given, by [15]

$$\hat{p}_e = p_e + \beta_p, \tag{78}$$

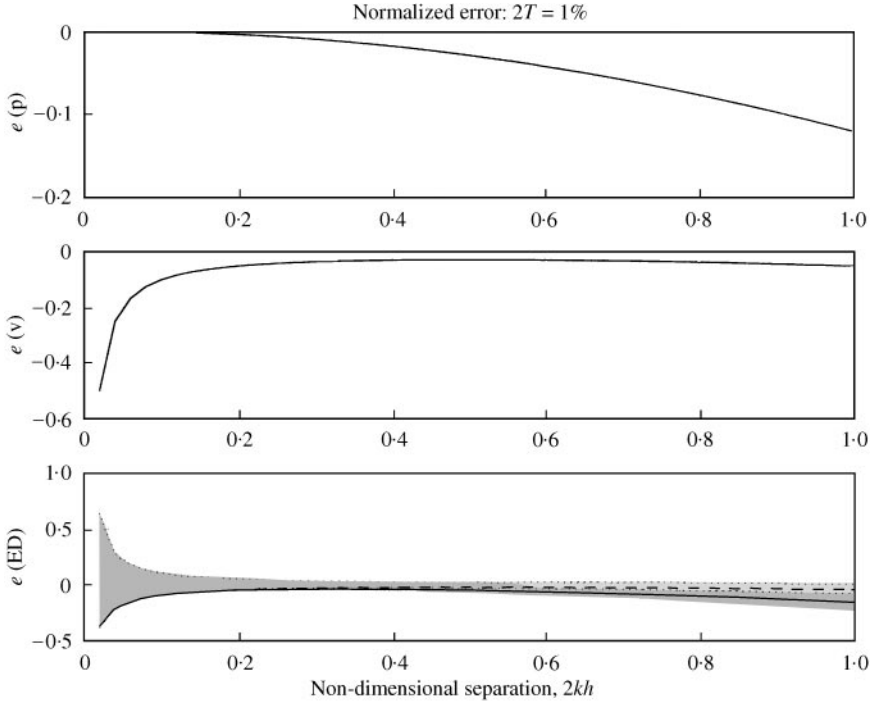

Figure 11. Normalized errors as a function of the non-dimensional separation distance ($2kh$) in a reactive one-dimensional sound field for a transducer sensitivity mismatch ($2T$) of 1% and $x/L = 1/4$: (a) pressure error $e(p)$, which is zero for the three-microphone sensor; (b) particle velocity error $e(v)$ which is the same for both sensors; (c) energy density error $e(ED)$, which is the same for both sensors for small kh. Maximum and minimum energy density error bands are shaded for the two-microphone sensor (dark grey) and the three-microphone sensor (light grey): —— 2-mic sensor; – – – – 3-mic sensor.

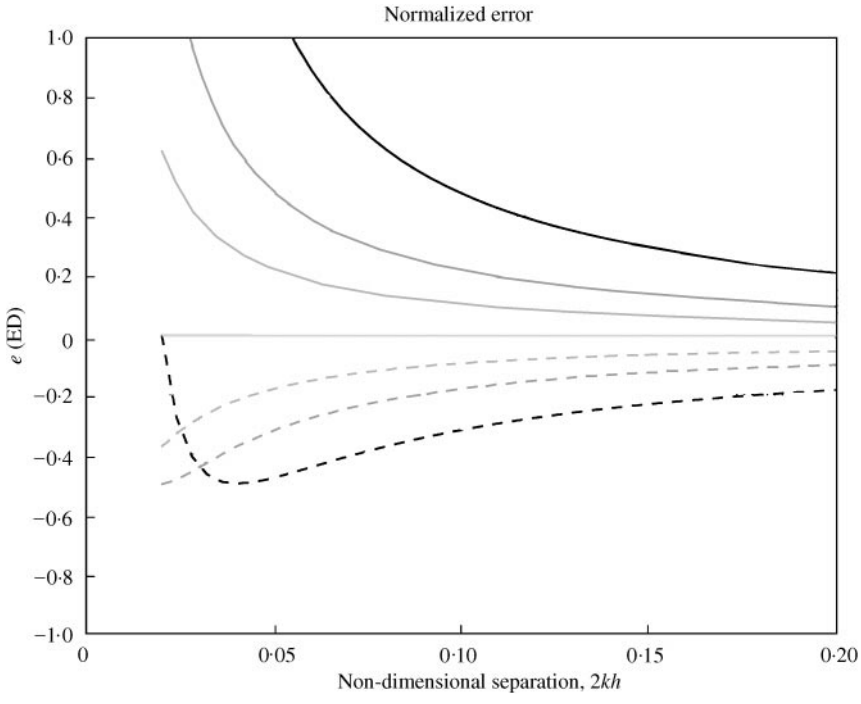

Figure 12. Normalized errors in energy density as a function of the non-dimensional separation distance ($2kh$) in a reactive one-dimensional sound field for several transducer sensitivity mismatches ($2T$) with $x/L = 1/4$: — -4%; — -2%; — -1%; — 0%; - - - 1%; - - - 2%; - - - 4%.

where β_p is the additional error due to the magnitude mismatch given by

$$\beta_p = \mathrm{j}PT\sin(kh) \approx \mathrm{j}hkPT\left[1 - \frac{(kh)^2}{6} + \frac{(kh)^4}{120} - \cdots\right]. \tag{79}$$

The normalized pressure error is therefore

$$e(\hat{p}) = e(p) + \mathrm{j}T\sin(kh) = [\cos(kh) - 1] + \mathrm{j}T\sin(kh). \tag{80}$$

Therefore, the sensitivity error introduces both a magnitude and phase error into the pressure estimate. The velocity estimate is given by [15]

$$\hat{v}_e = v_c + \beta_v, \tag{81}$$

where β_v is the additional error due to the magnitude mismatch given by

$$\beta_v = -\frac{T}{\mathrm{j}h\rho\omega}P\cos(kh) \approx -\frac{T}{\mathrm{j}h\rho\omega}P\left[1 - \frac{(kh)^2}{2} + \frac{(kh)^4}{24} - \cdots\right]. \tag{82}$$

The normalized velocity error is

$$e(\hat{v}) = e(v) + \mathrm{j}T\frac{\cos(kh)}{kh} = \left[\frac{\sin(kh)}{kh} - 1\right] + \mathrm{j}T\frac{\cos(kh)}{kh}. \tag{83}$$

As with the normalized pressure error, the sensitivity error introduces both a magnitude and phase error which becomes very large as kh approaches zero.

The energy density estimate is given by [15]

$$\hat{E}_{D_e} = E_{D_e} + \frac{P^2 T^2 \sin^2(kh)}{4\rho c^2} + \frac{T^2 P^2 \cos^2(kh)}{4\rho c^2 (kh)^2}. \tag{84}$$

The normalized error is thus,

$$e(\hat{E}_D) = e(E_D) + \frac{T^2}{2}\left(\sin^2(kh) + \frac{\cos^2(kh)}{(kh)^2}\right), \tag{85}$$

where $e(E_D)$ is the normalized error in the energy density without the phase mismatch arising wholly from the finite separation and is given by equation (47).

For small kh, equation (85) is approximately given by

$$e(\hat{E}_D) = e(E_D) + \frac{T^2}{2(kh)^2}. \tag{86}$$

The normalized error in the pressure, velocity and energy density is plotted against the non-dimensional separation distance in Figure 13 for a sensitivity mismatch of $2T = 1\%$. The effect of the sensitivity error is shown graphically in Figure 14 where the error in energy

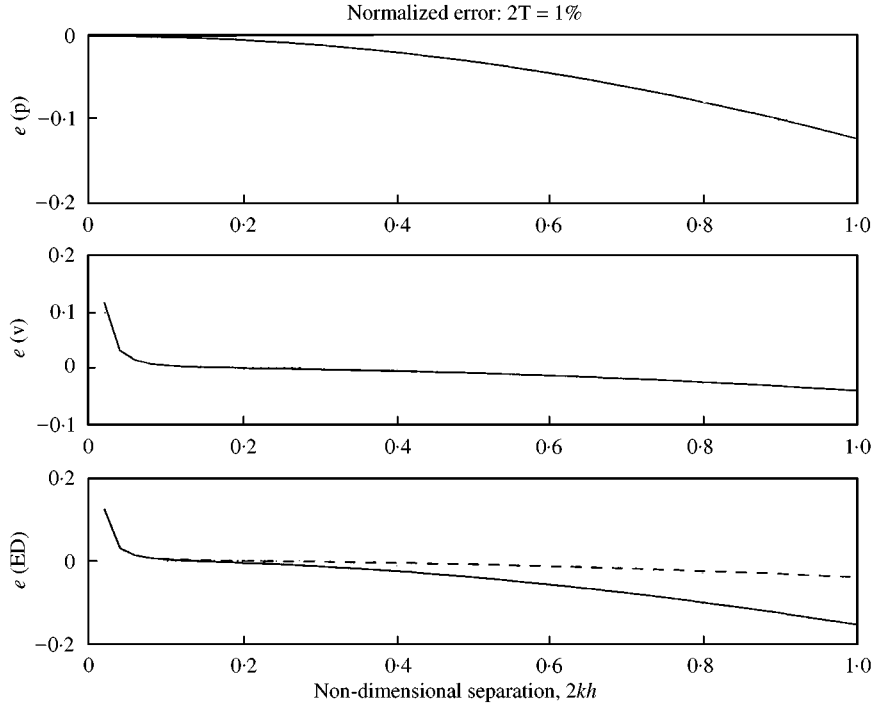

Figure 13. Normalized errors as a function of the non-dimensional separation distance ($2kh$) in a plane progressive sound field for a transducer sensitivity mismatch ($2T$) of 1%: (a) pressure error $e(p)$, which is zero for the three-microphone sensor; (b) particle velocity error $e(v)$ which is the same for both sensors; (c) energy density error $e(ED)$: —— 2-mic sensor; – – – – 3-mic sensor.

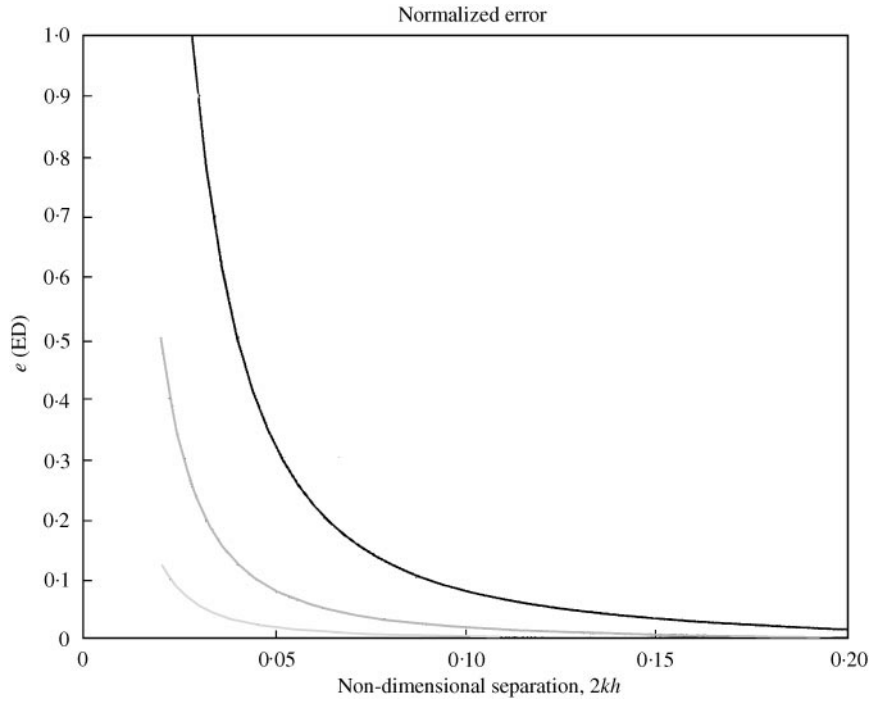

Figure 14. Normalized error in energy density as a function of the non-dimensional separation distance ($2kh$) in a plane progressive sound field for several transducer sensitivity mismatches ($2T$): 0%; 1%; 2%; 4%.

density given by equation (85) is plotted against non-dimensional separation distance for a variety of sensitivity errors.

Clearly, it is essential that the sensitivities of the two microphones are well matched and in practice, $2T < 1\%$ is certainly achievable.

For a three-microphone sensor, the pressure error is zero, the velocity error is the same as the two-microphone sensor given by equation (83) and the normalized error in the energy density estimate is given by the first and third terms of equation (85), i.e.,

$$e(\hat{E}_D) = e(E_{D_3}) + \frac{T^2}{2}\left(\frac{\cos^2(kh)}{(kh)^2}\right), \tag{87}$$

where $e(E_{D_3})$ is the inherent error for the three-microphone sensor given by equation (38).

3.2.3. *Length errors*

Because of manufacturing tolerances, the distance between acoustic centres of the microphones can vary. Typically, the accuracy may be in the order of $\pm$ 1 mm. It has been shown that length errors can lead to significant errors in intensity measurements [10, 13]. In the case of one-dimensional sound fields, it is only the length error component in the direction of energy flux that will cause errors in the estimates as shown in Figure 15. For example, if there is no spatial variation of pressure in the y direction, i.e., $\partial p/\partial y = 0$, then an error in the y-position, $\hat{y} = y + \varepsilon$, will not affect the pressure estimate, i.e., $p(\hat{y}) = p(y)$; however, an error in the x-position will.

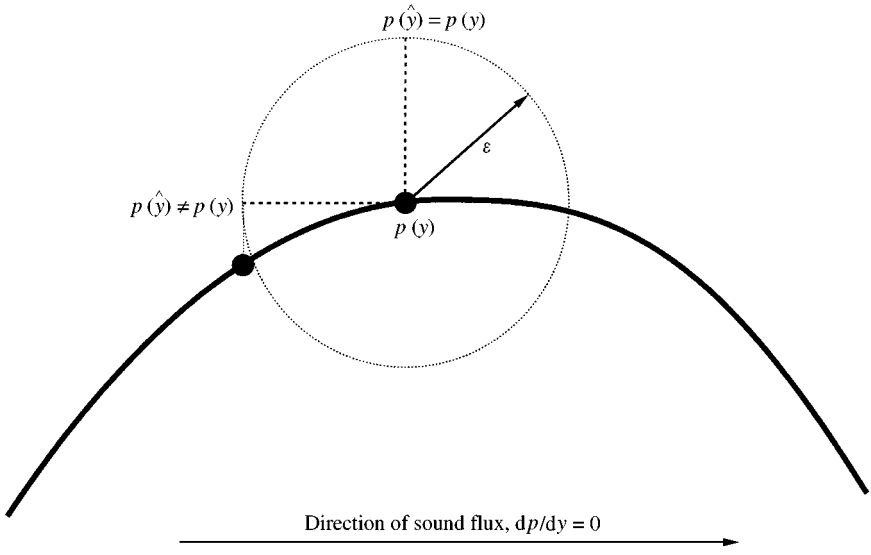

Figure 15. Effects of length error in the measurement of pressure at a point.

The effects, of length errors will now be analyzed for two types of idealized sound fields using a symmetric formulation for the spatial error as was done for the phase and sensitivity mismatches. It can be shown that the additional error arising from the symmetric formulation as compared to a non-symmetric formulation is second order and may be neglected.

3.2.3.1. One-dimensional reactive sound field. If the error in position is given by $\pm\varepsilon$, then the non-dimensional spacing is given by $k\hat{h} = kh + k\varepsilon$ or $\hat{h}/h = 1 + k\varepsilon/kh$. The normalized error for the pressure, velocity and energy density estimates are therefore given by [15]

$$e(\hat{p}) = \cos(k\hat{h}) - 1 \approx -\frac{(k\hat{h})^2}{2} + \frac{(k\hat{h})^4}{24} - \frac{(k\hat{h})^6}{720} + \cdots, \tag{88}$$

$$e(\hat{v}) = \frac{\sin(k\hat{h})}{kh} - 1 \approx \left(1 + \frac{k\varepsilon}{kh}\right)\left(1 - \frac{(k\hat{h})^2}{6} + \frac{(k\hat{h})^4}{120} - \frac{(k\hat{h})^6}{5040} + \cdots\right) - 1, \tag{89}$$

$$e(\hat{E}_D) \approx \cos^2(kx)\left[1 - (k\hat{h})^2 + \frac{(k\hat{h})^4}{3}\right] + \sin^2(kx)\left(\frac{k\hat{h}}{kh}\right)^2\left[1 - \frac{(k\hat{h})^2}{3} + \frac{2(k\hat{h})^4}{45}\right] - 1. \tag{90}$$

Using $\hat{h}/h = 1 + k\varepsilon/kh$, the normalized error for the energy density estimate is

$$e(\hat{E}_D) \approx \cos^2(kx)\left[1 - (k\hat{h})^2 + \frac{(k\hat{h})^4}{3}\right] + \sin^2(kx)\left(1 + \frac{k\varepsilon}{kh}\right)^2\left[1 - \frac{(k\hat{h})^2}{3} + \frac{2(k\hat{h})^4}{45}\right] - 1. \tag{91}$$

The error in transducer position produces almost no change in the error for the pressure estimate. However, the velocity estimate is biased by ε/h and the energy density error is biased by approximately $2\varepsilon/h \sin^2(kx)$.

From equation (91) it can be seen that for small kh the minimum energy density error occurs at $kx = n\pi$ and is approximately given by $e(\hat{E}_D)_{min} = e(E_D)$, which is the error arising from only the finite microphone separation. The maximum error in the energy density estimate is found at $kx = (2n + 1)\pi/2$,

$$e(\hat{E}_D)_{max} = e(E_D) + 2\frac{\varepsilon}{h}. \tag{92}$$

The truncated Taylor series expansions for the normalized error in pressure, velocity and energy density as given by equations (88)–(90) using a 4% error in the transducer location are plotted against the non-dimensional separation distance in Figure 16, with a non-dimensional position of $x/L = \frac{1}{4}$.

The normalized error in the energy density given by equation (91) is shown graphically in Figure 17 where the error is plotted against non-dimensional separation distance for a variety of length errors.

For a three-microphone sensor, for small kh the error in energy density is given by

$$e(\hat{E}_D) \approx \cos^2(kx) + \sin^2(kx)\left(1 + \frac{k\varepsilon}{kh}\right)^2\left[1 - \frac{(k\hat{h})^2}{3} + \frac{2(k\hat{h})^4}{45}\right] - 1. \tag{93}$$

Therefore, the additional microphone does not greatly assist in reducing the low-frequency error resulting from length effects in a reactive sound field.

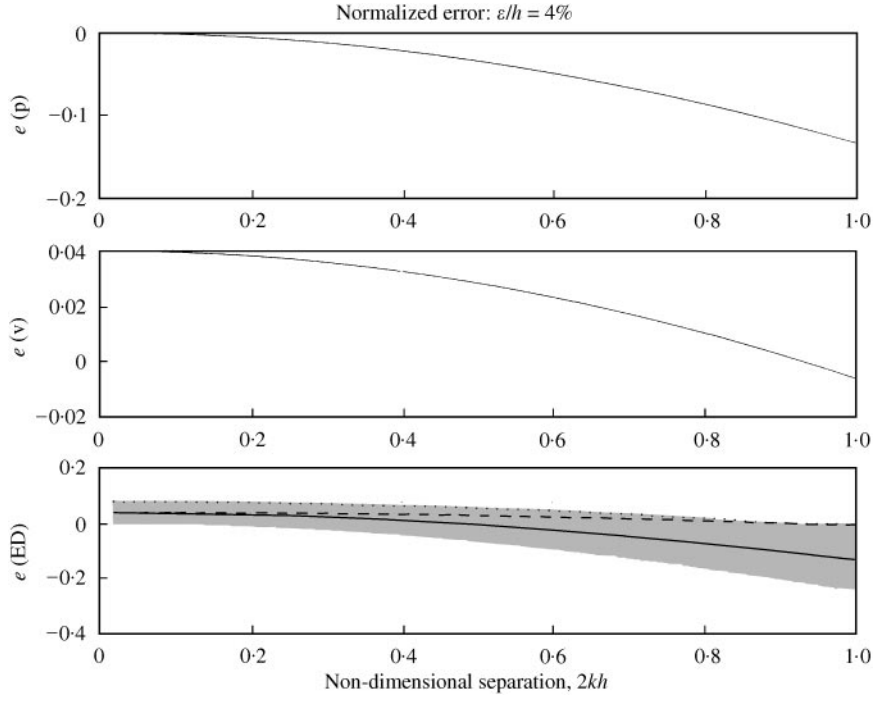

Figure 16. Normalized errors as a function of the non-dimensional separation distance ($2kh$) in a reactive one-dimensional sound field for a $\varepsilon/h = 4\%$ error in the transducer position with $x/L = 1/4$: (a) pressure error $e(p)$ which is zero for the three-microphone sensor; (b) particle velocity error $e(v)$ which is the same for both sensors; (c) energy density error $e(ED)$ which is approximately the same for both sensors for small kh. Maximum and minimum energy density error bands are shaded for the two-microphone sensor (dark grey) and the three-microphone sensor (light grey) which is hidden: —— 2-mic sensor; ···· 3-mic sensor.

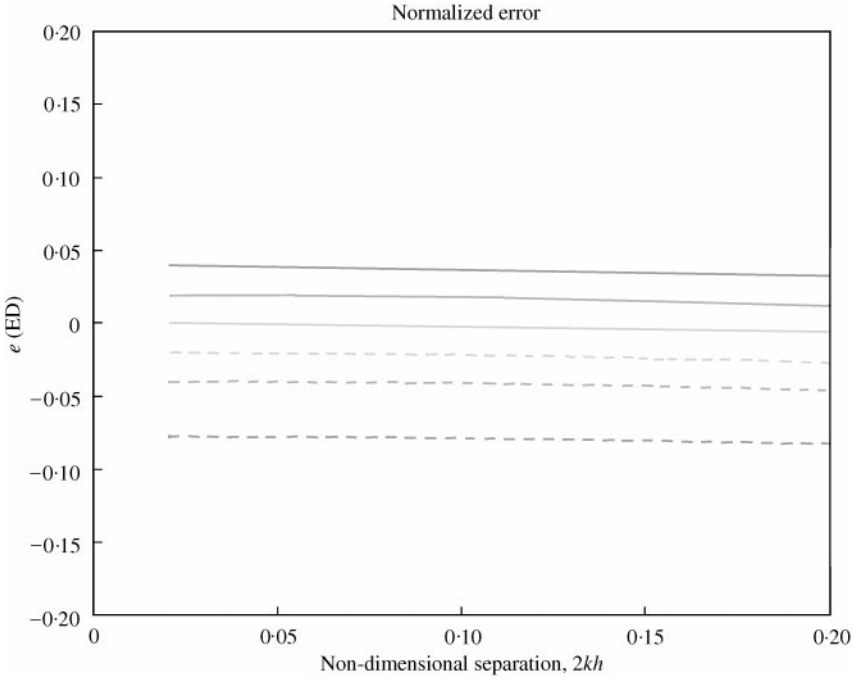

Figure 17. Normalized error in the energy density estimate as a function of the non-dimensional separation distance ($2kh$) in a reactive one-dimensional sound field for several transducer position errors with $x/L = 1/4$: - - - 8%; - - - 4%; - - - 2%; —— 0%; —— 2%; —— 4%; —— 8%.

3.2.3.2. Plane progressive wave. In the case of a plane wave the effect of an error in the length is the same as a phase mismatch. For a length error of 2ε then $k\hat{h} = kh + k\varepsilon$ or $\hat{h}/h = 1 + k\varepsilon/kh$. The normalized errors for the pressure, velocity and energy density are given by [15]

$$e(p) = \cos(k\hat{h}) - 1 \approx -\frac{(k\hat{h})^2}{2} + \frac{(k\hat{h})^4}{24} - \frac{(k\hat{h})^6}{720} + \cdots, \tag{94}$$

$$e(v) = \frac{\sin(k\hat{h})}{kh} - 1 \approx \left(1 + \frac{k\varepsilon}{kh}\right)\left(1 - \frac{(k\hat{h})^2}{6} + \frac{(k\hat{h})^4}{120} - \frac{(k\hat{h})^6}{5040} + \cdots\right) - 1, \tag{95}$$

$$e(\hat{E}_D) \approx \frac{1}{2}\left[1 - (\hat{h}k)^2 + \frac{1}{3}(\hat{h}k)^4\right] + \frac{(1 + k\varepsilon/kh)^2}{2}\left[1 - \frac{1}{3}(\hat{h}k)^2 + \frac{2}{45}(\hat{h}k)^4\right] - 1. \tag{96}$$

As was the case for the reactive sound field, the pressure estimate changes very little, the velocity is biased by ε/h and the energy density error is also biased by ε/h for small ε/h since $(1 + \varepsilon/h)^n \approx 1 + n\varepsilon/h$. Therefore, the effect of the spacing error is to increase the finite difference error by a factor of approximately ε/h which can be seen in Figure 18 for an error of 4%.

The normalized error in the energy density given by equation (96) is shown graphically in Figure 19 where the error is plotted against non-dimensional separation distance for a variety of length errors.

For a three-microphone sensor the normalized errors are given by the errors arising from a phase mismatch with $\phi_s = k\varepsilon$. The normalized error in the pressure is clearly zero, the

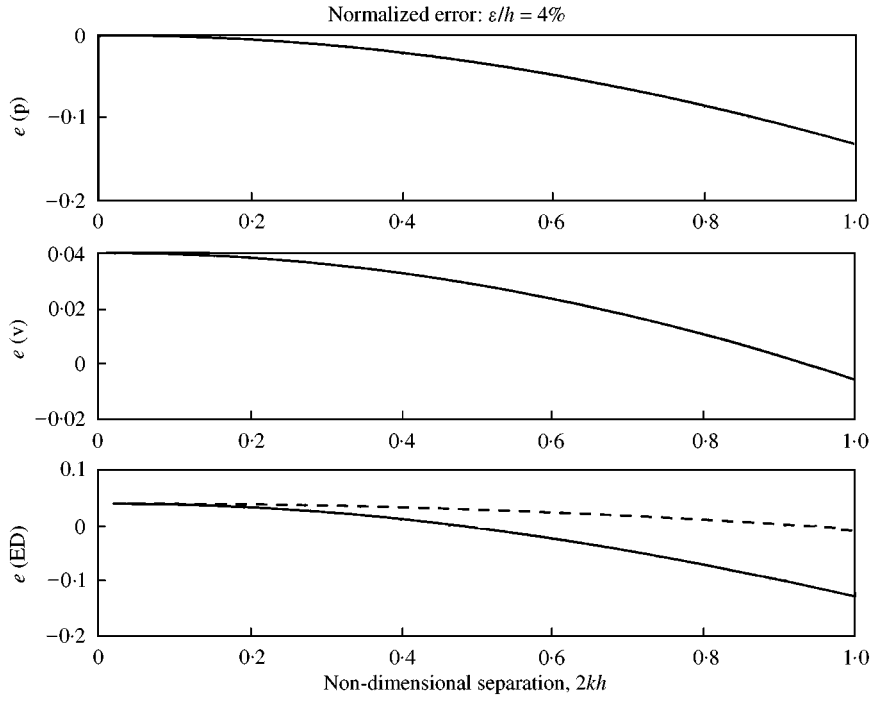

Figure 18. Normalized errors as a function of the non-dimensional separation distance ($2kh$) in a free progressive sound field for a $\varepsilon/h = 4\%$ error in the transducer position: (a) pressure error $e(p)$, which is zero for the three-microphone sensor; (b) particle velocity error $e(v)$, which is the same for both sensors; (c) energy density error $e(ED)$, which is the same for both sensors for small kh: —— 2-mic sensor; – – – – 3-mic sensor.

error for the velocity is the same as for the two-microphone sensor given by equation (95) and the normalized error in the energy density is given by the second term in equation (96), i.e.,

$$e(\hat{E}_{D_3}) \approx \frac{(1 + k\varepsilon/kh)^2}{2}\left[1 - \frac{1}{3}(\hat{h}k)^2 + \frac{2}{45}(\hat{h}k)^4\right] - \frac{1}{2}. \tag{97}$$

Therefore, since it is the ε/h bias error arising from the $(1 + k\varepsilon/kh)^2$ term that dominates the error in the energy density estimate at low frequencies, it can be concluded that the use of the additional microphone does not reduce the bias error in the energy density resulting from length errors in a progressive plane wave.

3.3. OTHER ERROR SOURCES

3.3.1. *Different and interference effects at the microphones*

Diffraction and interference effects arising from the finite size of the closely spaced microphones are extremely difficult to estimate. The effect becomes more important at very high frequencies where it results in large phase deviations. Fortunately, at the same time, the phase deviations at high frequencies have less influence over the accuracy (see section on phase and sensitivity errors).

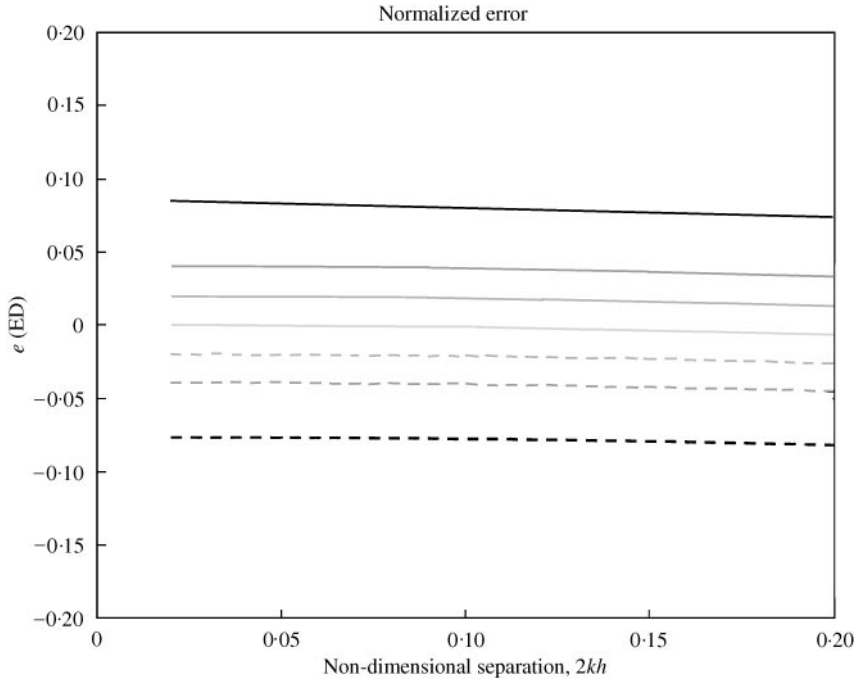

Figure 19. Normalized error in the energy density estimate as a function of the non-dimensional separation distance ($2kh$) in a free progressive sound field for several transducer position errors ε/h: – – – 8%; – – – 4%; – – – – – – 2%; —— 0%; —— 2%; —— 4%; —— 8%.

Based on previous research on the obstacle effects on the measurement of sound intensity [3,7,9], the errors are thought to be negligible within the frequency range of most active noise control applications (60–600 Hz) and will not be considered here. Naturally, the more solid material used the greater the effects of diffraction and therefore the design should aim to minimize the solid bulk of the energy density sensor.

3.3.2. *Mean flow and turbulence*

According to Fahy [13], strictly speaking, the two-microphone technique used for the sensing of particle velocity is invalid in the presence of mean flow, however small, because it is based on the zero mean flow momentum equation. It can be shown that in the presence of mean flow with Mach number, M, the momentum equation becomes [13]

$$\frac{\partial p}{\partial x} = -\mathrm{j}\omega\rho_0 u(1 - M), \tag{98}$$

where u is the particle velocity due to the acoustic field. Therefore, the error in the energy density will be small if $M \ll 1$. It should be noted that the mean flow may arise from exposure of the sensor to vibrations and hence should be avoided.

In any measurements in the presence of mean flow there will always be unsteady components acting on the microphones which can lead to errors. Therefore, the sensor must be protected from the effects of turbulence, which is commonly achieved with the use of foam windshields.

3.3.3. *Environmental effects*

For the two-microphone technique to work effectively in a range of environments it is essential that the microphones used are stable over a range of temperatures and humidities. Obviously, sensors used in stable environments such as laboratories can tolerate temperature and humidity sensitivities, whereas sensors used on site require highly stable microphones.

3.3.4. *Statistical or random errors*

Random errors are not influenced by the specific measurement situation and may arise from electrically generated random noise, turbulent flow and local vibrations on the instrument [10,13]. The random error in the transfer function estimate between two microphones is given by [10]

$$\varepsilon_r(|H_{12}|) \approx \sqrt{\frac{1-\gamma_{12}^2}{2n\gamma_{12}^2}}, \qquad \sigma(\Phi_{12}) \approx \varepsilon_r(|H_{12}|), \tag{99, 100}$$

where ε_r is the normalized random error in the transfer function, γ_{12}^2 equals the coherence between the signals from the two microphones, n is the number of averages and σ is the standard deviation of the transfer function in radians. It is evident from the above equations that in order to keep the random errors small, the coherence must be kept high. In practice, the coherence between microphones with small spacings is always high ($\gamma^2 > 0{\cdot}9$) and subsequently, the error in the transfer function between the microphones is low.

While random errors may be an issue for the measurement of time-averaged sound intensity it is not a significant issue for the use of energy density as an error signal. This is particularly true in a feedforward control system, where the effects of uncorrelated random noise are negligible on the calculation of the optimum phase and magnitude of the control sources. However, the noise does reduce the dynamic range of the system and if the noise signal becomes large compared to the signals due to the primary field then this may limit the reduction that can be achieved. If care is taken, then the effect of these random errors are inconsequential and subsequently, these effects were not thoroughly investigated here. Even for feedback systems (which are only effective at controlling noise with a reasonably high auto-correlation coefficient) it is not expected that this type of error will reduce the level of control significantly provided that good signal-to-noise ratios are maintained.

3.4. SUMMARY

It should be noted that in practice a variety of errors will occur in the measurement of the energy density and the resulting normalized errors are not simply additive but rather the errors become compounded in a very complicated fashion and are heavily dependent on the sound field characteristics. It can be said however, that the above analysis does provide an indication of the magnitude of the errors to be expected from a typical sensor operating in two idealized sound fields. Table 1 presents a summary of the typical errors experienced during the measurement of energy density.

Table 1 can be used to define the frequency bounds for a sensor. For example, let the permissible normalized error in the energy density be 10% and the operating range be the decade 60–600 Hz. For a reactive sound field, the location of the sensor in the field determines the size of the error, so it is important to use the largest error in the field. The upper frequency limit (restricted by the inherent error) defines the largest size that the sensor may be i.e., $2h < 57$ mm. All other instrumentation errors determine the smallest size that

TABLE 1

Summary of approximate normalized errors in energy density, $e(E_D)$, where $2kh$ is the non-dimensional spacing between microphones, kx is the position in the reactive sound field, $2\phi_s$ is the phase error, $2T$ is the error in the sensitivity and 2ε is the error in the location of the microphones

Error type	Low-frequency limit		High-frequency limit	
	Reactive field	Plane wave	Reactive field	Plane wave
Inherent	0	0	$-(kh)^2\left[\dfrac{2\cos^2(kx)+1}{3}\right]+\cdots$	$-\dfrac{2}{3}(kh)^2+\cdots$
Phase	$\cos^2(kx)\left(\dfrac{2\phi_s}{2kh}\right)^2$	$-\dfrac{2\phi_s}{2kh}+\dfrac{1}{2}\left(\dfrac{2\phi_s}{2kh}\right)^2$	$-(kh)^2\left[\dfrac{2\cos^2(kx)+1}{3}\right]+\cdots$	$-\dfrac{2}{3}(kh)^2+\cdots$
Sensitivity	$-\left(\dfrac{2T}{2kh}\right)\sin(2kx)+\left(\dfrac{2T}{2kh}\right)^2\cos^2(kx)$	$\dfrac{1}{2}\left(\dfrac{2T}{2kh}\right)^2$	$-(kh)^2\left[\dfrac{2\cos^2(kx)+1}{3}\right]+\cdots$	$-\dfrac{2}{3}(kh)^2+\cdots$
Position	$\cos^2(kx)+\sin^2(kx)\left(1+2\dfrac{2\varepsilon}{2h}\right)-1$	$\dfrac{2\varepsilon}{2h}$	$-(kh)^2\left[\dfrac{2\cos^2(kx)+1}{3}\right]+\cdots$	$\dfrac{2\varepsilon}{2h}-\dfrac{2}{3}(kh)^2+\cdots$

the sensor may be. For a phase error of $2\phi_s = 1^\circ$, then $2h > 50$ mm. For a sensitivity error of $2T = 0{\cdot}5\%$, then $2h > 45$ mm. For a position error of $2\varepsilon = 2$ mm, then $2h > 40$ mm. A suitable compromise for such a design may be $2h = 50$ mm. This in fact has formed the basis of the design of several 3D energy density sensor configurations studied by the authors in the companion paper [14].

4. CONCLUSIONS

An expression has been derived for the energy density estimate in ideal one-dimensional sound fields using two or three microphones. The errors in the energy density estimate arising from several sources were considered; inherent errors (finite differance and finite sum), phase errors, sensitivity errors, length errors, diffraction and interference effects, and other error sources such as temperature and humidity.

The inherent errors were found to limit the upper frequency range of the energy density sensor, and the instrumentation (phase and sensitivity) errors where found to define the low-frequency limit.

ACKNOWLEDGMENTS

The authors gratefully acknowledge the financial support for this work provided by Australian Research Council and the Sir Ross & Keith Smith Fund.

REFERENCES

1. S. D. Sommerfeldt and P. J. Nashif 1991 *Proceedings of Noise-Con* 91, 299–306. A comparison of control strategies for minimising the sound field in enclosures.
2. G. Pavic 1977 *Journal of Sound and Vibration* **51**, 533–545. Measurement of sound intensity.
3. S. J. Elliott 1981 *Journal of Sound and Vibration* **78**, 439–445. Errors in acoustic intensity measurements.
4. J. K. Thompson and D. R. Tree 1981 *Journal Sound and Vibration* **75**, 229–238. Finite difference approximation errors in acoustic intensity measurements.
5. J. K. Thompson 1982 *Journal Sound and Vibration* **82**, 459–464. Comments on "Finite difference approximation errors in acoustic intensity measurements".
6. J. K. Thompson 1982 *Proceedings of Inter Noise* 82, 723–726. Acoustic intensity measurement error.
7. P. Kitech and J. Tichy 1982 *Proceedings of Inter Noise*, 695–698. Intensity probe obstacle effects and error of the transfer function technique to calibrate acoustic intensity measurements.
8. J. C. Pascal and C. Carles 1982 *Journal of Sound and Vibration* **83**, 53–65. Systematic measurement errors with two microphone sound intensity meters.
9. G. Krishnappa 1983 *Noise Control Engineering Journal* **21**, 126–135. Interfence effects in the two microphone technique of acoustic intensity measurements.
10. H. Boden and M. Abom 1986 *Journal of the Acoustical Society of America* **79**, 541–549. Influence of errors on the two-microphone method for measuring acoustic properties in ducts.
11. P. S. Watkinson 1986 *Journal of Sound and Vibration* **105**, 255–263. The practical assessment of errors in sound intensity measurement.
12. G. W. Elko 1991 *Proceedings of Noise-Con* 91, 541–546. Biased against finite-difference bias.
13. F. Fahy 1995 *Sound Intensity*. London: E&FN Spon, second edition.
14. B. S. Cazzolato and C. H. Hansen 1999 *Journal of Sound and Vibration* **236**, 375–400. Errors arising from three-dimensional acoustic energy density sensing in one-dimensional sound fields.
15. B. S. Cazzolato 1999 *Ph.D. dissertation, The University of Adelaide, March*. Sensing systems for active control of sound transmission into cavities.
16. P. J. Nashif and S. D. Sommerfeldt 1992 *Proceedings of Inter Noise* 92, 357–361. An active control strategy for minimising the energy density in enclosures.